Journal of Alloys and Compounds 499 (2010) 238–242

Contents lists available at ScienceDirect

Journal of Alloys and Compounds

journal homepage: www.elsevier.com/locate/jallcom

Effect of melting time on the superconductivity in $Bi_{1.7}Pb_{0.3}Sr_2CaCu_2O_8$ superconducting system

A. Sedky*,[1]

Physics Department, Faculty of Science, King Faisal University, P.O. Box 400, Al-Hassa 31982, Saudi Arabia

ARTICLE INFO

Article history:
Received 25 January 2010
Received in revised form 17 March 2010
Accepted 18 March 2010
Available online 25 March 2010

Keywords:
Synthesis
Characterization
Bi: 2212
Excess oxygen and melting operation

ABSTRACT

We reported here the effect of melting time (1.5–5 min + 5 s) in air and at 920 °C on the normal and superconducting properties of $Bi_{1.7}Pb_{0.3}Sr_2CaCu_2O_8$ (Bi (Pb): 2212) system. The results of X-ray diffraction, microhardness, resistivity and Hall effect are presented in details. Furthermore, the superconducting critical temperature T_c, normal resistivity ρ_{300}, residual resistivity ρ_0, and resistivity slope corresponding to the linear ρ-T region and width of transition ΔT_c are extracted from resistivity data. Moreover, various normal state parameters, such as density of holes, Fermi energy and density of states at the Fermi level are calculated for all samples. These results shows a correlation between the above measured parameters against melting time, and indicate that 3.5 min is the suitable melting time to optimizing T_c at 89 K for Bi (Pb): 2212 superconducting system.

1. Introduction

Since the discovery of BSCCO superconductors by Maeda [1], extensive research efforts have been directed towards the correlation between its synthesis and superconductivity. It is found that optimum doping levels in Bi: 2212 system can be controlled either by changing the amount of excess oxygen or by the chemical substitution [2–4]. Recently, scanning tunneling spectroscopic studies for Bi: 2212 system have observed spatially inhomogeneous electronic states [5], but it is not clear whether this behavior is originally due to chemical doping or oxygen disorder [6]. However, it has been recognized that the superconductivity of such system is closely related to the excess oxygen which is introduced during synthesis, and the critical temperature T_c could be optimized by removing a part of excess oxygen through proper annealing [7], and consequently the hole concentration per Cu ion may be affected [2,8]. On the other hand, a reduction of Bi valence state by Pb substitution gives rise to electronic conduction in the Bi–O layers of Bi (Pb) SCCO superconducting system, whereas the oxidation of Cu gives rise to hole conduction in $Cu–O_2$ planes of such system [9–11]. Usually, it is not possible to ensure that the system is properly optimized or not. Furthermore, the systematic study based on both excess oxygen and Pb substitution with regard to hole concentration in Bi (Pb): 2212 system are not well understood [12].

However, lots of work has been made for obtaining $Bi_{1.7}Pb_{0.3}Sr_2CaCu_2O_8$ [Bi (Pb): 2212] high T_c system [13–17]. Normally, this high T_c cuprates possesses the T_c of (73–87 K) [18,19]. Agrawal et al. have been succeeded in raising T_c up to 91 K by incorporating the quenching process [13]. The quenching as well as melting processes are primarily known to reduce the excess oxygen of Bi: 2212 system. Unlikely the quenching process, the melting point cannot be detected exactly by different scientist and always leads to different values of T_c for the samples prepared under the same conditions. In the present work, we report the synthesis of Bi (Pb): 2212 samples obtained through melting operation, without any nitrogenated heat treatment. For simplicity, we fixed Pb content at 0.30 and put our attentions for studying the impact of melting operation on superconductivity for the considered system. Our results shows that the melting time can optimize the superconductivity of Bi (Pb): 2212 system due to its impact on excess oxygen produced through melting operation as well as quenching process.

2. Experimental details

$Bi_{1.7}Pb_{0.3}Sr_2CaCu_2O_8$ samples are prepared by the well-known solid-state reaction method. The ingredients of Bi_2O_3, PbO, SrO, $CaCO_3$ and CuO with 4N purity are thoroughly well mixed in the required compositions and calcined at 820 °C for 24 h. This procedure is repeated three times with intermediate grinding at each stage. The resulting powder is reground and pelletized into equally six pellets. The prepared samples are separately brought to a partially melting state at 920 °C and at different six values of time as follows: 1.5, 2.5, 3.5, 4, 4.5 and 5 min + 5 s), respectively. 5 s is the time taken to shift the sample from furnace. Then, the samples are cooled to room temperature with an intervening annealing in air at 870 °C for 24 h. The samples are then characterized for phase purity at room temperature (300 K) by X-ray diffraction with Cu Kα radiation. The lattice parameters are calculated by

* Permanent address: Physics Department, Faculty of Science, Assiut University, Assiut, Egypt.
E-mail address: sedky1960@yahoo.com.
[1] Tel.: +966 507207331; fax: +966 35886437.

0925-8388/$ – see front matter © 2010 Elsevier B.V. All rights reserved.
doi:10.1016/j.jallcom.2010.03.175

Table 1
Lattice parameters, Hall coefficient, density of holes, Fermi energy and density of states versus melting time for Bi (Pb): 2212 samples.

Melting time (min)	a (Å)	c (Å)	R^{-1} (C/cm^{-3})	n (cm^{-3})	E_f (eV)	$N(E_f)$ [state/eV cm^3]
1.5	5.403	30.790	346.02	2.16×10^{21}	0.132	12.69×10^{33}
2.5	5.406	30.842	440.53	2.75×10^{21}	0.153	13.73×10^{33}
3.5	5.411	30.911	662.25	4.15×10^{21}	0.198	15.71×10^{33}
4	5.409	30.880	552.49	3.47×10^{21}	0.176	14.82×10^{33}
4.5	5.408	30.855	536.57	3.37×10^{21}	0.171	13.56×10^{33}
5	5.407	30.844	520.65	3.27×10^{21}	0.166	13.17×10^{33}

using computer programme and in terms of Bragg peaks over the 2θ range. Surface morphology of the samples is performed by scanning electron microscope (SEM). The room temperature microhardness of the samples are determined using an MH-6 digital microhardness tester (0.098–9.8 N). The Vickers microhardness (VHN) is estimated according to the following equation:

$$\mathrm{VHN} = 0.1891 \left(\frac{P}{d^2}\right)$$

where P is the applied load (in N) and d is the diagonal length of indentor impression. The electrical resistivity of the samples is measured by the standard four-probe technique in closed cycle refrigerator within the range of (20–300 K) [cryomech compressor package with cryostat Model 810-1812212, USA]. Nanovoltameter Keithley 2182, current source Keithley 6220 and temperature controller 9700 (0.001 K resolution) are used in this experiment. Finally, the Hall coefficients for the samples are measured at room temperature using Ecopia HMS-2000/0.55 T.

3. Results and discussion

3.1. Structural and mechanical analysis

Fig. 1 shows the room temperature XRD patterns of selected four Bi (Pb): 2212 samples. It is clear that all diffractograms shows the characteristic lines of Bi: 2212 tetragonal single phase and some few peaks are related to Bi: 2201 phase. No extra peaks are observed in the patterns for all samples. In addition, there is a little variation of the lines intensity of all peaks with melting time, which could be related to the observed change in the T_c values presented in the next section. The marginal shift in the position of lines is attributed to the change in the c-lattice parameter. Moreover, there is no indication for orthorhombic–tetragonal lines splitting in all diffractograms.

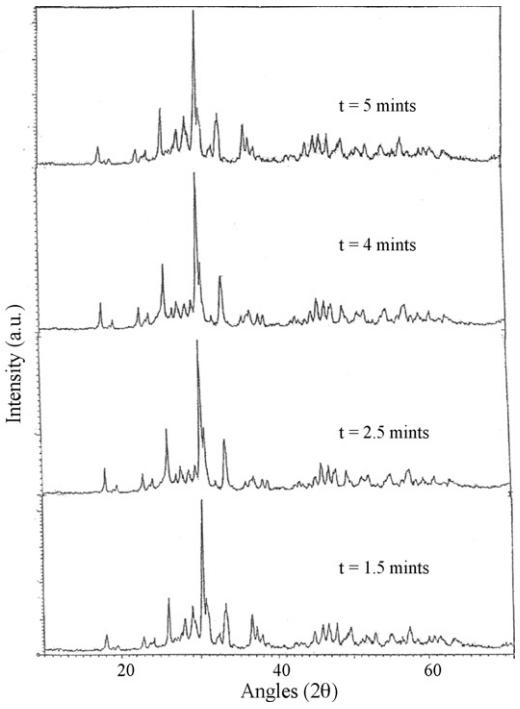

Fig. 1. Room temperature X-ray diffraction patterns versus melting. Time for Bi (Pb): 2212 samples.

The variation of lattice parameters a and c against melting time for all considered samples are listed in Table 1. It is evident from the table that lattice parameters are slightly increased with increasing melting time from 1.5 min up to 3.5 min followed by a decrease with further increase of time up to 5 min. The lattice parameters obtained in the present work are in good agreement with those reported earlier [7,20–22]. The behavior of lattice parameters against melting time is probably related to the change in the coupling between Cu–O planes produced by the amount of excess oxygen during melting operation, which is responsible for the T_c variation [21]. The change of excess oxygen with melting time up to 3.5 min leads to increasing c-parameter, and consequently the spacing between CuO_2 planes is increased. The vice versa with further increase of the melting time.

Surface morphology of Bi: 2212 samples is shown in Fig. 2(a)–(f). In 1.5 min sample, the size of grains is not homogenous along with a random precipitation on the mother grains. The black regions are randomly distributed in the matrix structure with a few microcracks propagates along the grain boundaries, which indicates a weaker link between the grains. Few small black lumps are dispersed in the matrix, which may be related to some non-superconducting phases. With increasing time up to 3.5 min, the grains are uniformly distributed with a few dark regions propagates along the grain boundaries. Also, the size of white grains is increased, which indicates a strong connection between them. With further increase of melting time up to 5 min, the grains appear with relatively large size, which is responsible for the low-T_c.

Behavior of microhardness (VHC) against melting time shown in Fig. 3 is typically similar to the behavior of lattice parameters (Table 1). The highest value of VHC recorded at $t = 3.5$ min is probably attributed to the improvement of the coupling between grains and elimination of pores, which occurs during melting operation. Then, one can say that the mechanical resistance (the resistance of material to the applied mechanical load) at this period becomes higher and consequently the mechanical connection is improved. On the other hand, it can be concluded that the higher microhardness values measured at lower loads (0.098 N) represent the hardness of monocryatalline grains, whereas the lower values measured at higher loads (4.9 N) usually represent the crack patterns and crack propagation along grain boundaries [16].

3.2. Resistivity and Hall coefficient

Electrical resistivity versus temperature curves of Bi (Pb): 2212 samples are presented in Fig. 4(a). In general the $\rho(T)$ curves involve a normal state region, which extends from room temperature down to a temperature close to onset temperature T_{on}. The $\rho(T)$ curves has a slope ($d\rho/dT$) which is connected with carrier–carrier scattering, and the extrapolation of $\rho(T)$ to $T = 0$ K provides the residual resistivity, say, ρ_0 which is connected with impurity scattering [23]. The values of both ρ_{300} and ρ_0 are drawn as a function of melting time and shown in Fig. 4(b). It is clear that ρ_{300} and ρ_0 decrease with increasing melting time up to 3.5 min, followed by an increase with further increase of time up to 5 min. This behavior indicates that the electron scattering by impurities is also affected by melting time as well as in the case of normal state resistivity ρ_{300}. The

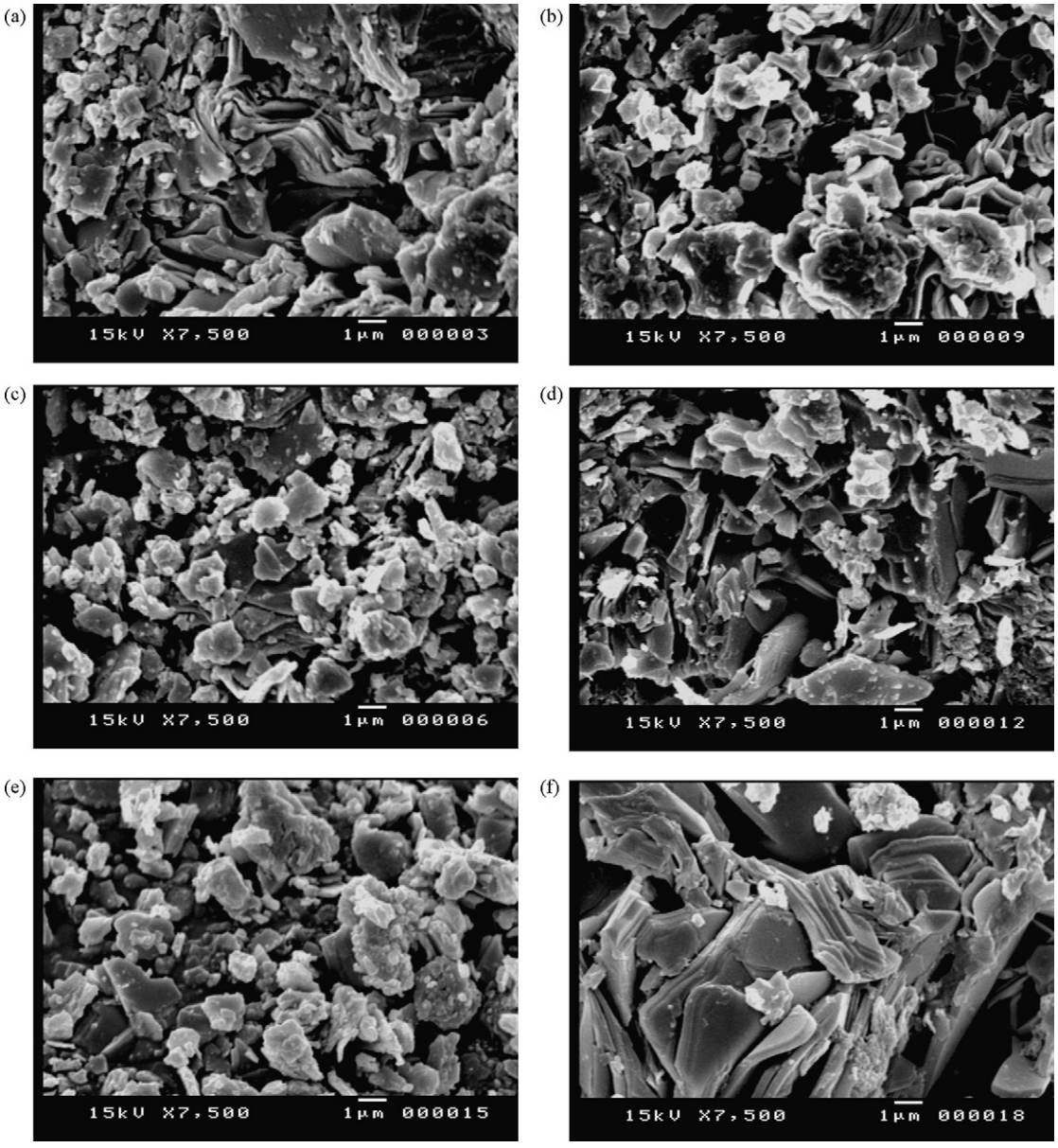

Fig. 2. (a) SEM photograph of pure Bi: 2212 sample (t = 1.5 min). (b) SEM photograph of pure Bi: 2212 sample (t = 2.5 min). (c) SEM photograph of pure Bi: 2212 sample (t = 3.5 min). (d) SEM photograph of pure Bi: 2212 sample (t = 4 min). (e) SEM photograph of pure Bi: 2212 sample (t = 4.5 min). (f) SEM photograph of pure Bi: 2212 sample (t = 5 min).

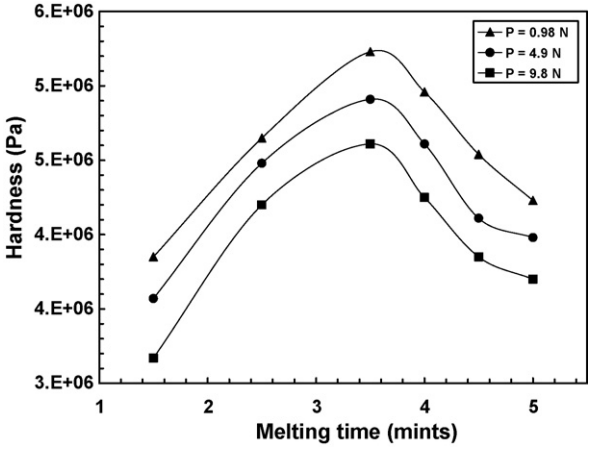

Fig. 3. Microhardness versus melting time for Bi (Pb): 2212 samples.

($d\rho/dT$) behavior shown in Fig. 4(c) indicates that all samples has a negative slope except the samples melted at t = 2.5 and 3.5 min, where the slope is positive for these two samples. This means that the behavior is metallic only for these two samples, and rest of the samples shows semiconductor behavior, as the slope in negative for the rest of samples. The behaviors of both T_c, T_{on} and width of transition ΔT_c as a function of melting time are shown in Fig. 4(d). [$\Delta T_c = (T_{on} - T_c)$ is the temperature width from onset temperature T_{on} down to critical temperature T_c]. It is found that both T_c and T_{on} are increased with increasing melting time up to 3.5 min followed by a decrease of their values with further increase of melting time up to t = 5 min. The values of T_c are 40, 66, 89, 75, 68 and 52 K for all samples and the values of ΔT_c are 45, 14, 4, 20, 22 and 28 K for the samples melted at t = 1.5, 2.5, 3.5, 4, 4.5 and 5 min, respectively. These values means that the transition of the sample molten at t = 3.5 min becomes sharper (ΔT_c = 4 K) and T_c goes higher up to 89 K, in agreement with the above analysis for structural and microhardness. The behavior of the above parameters against melting

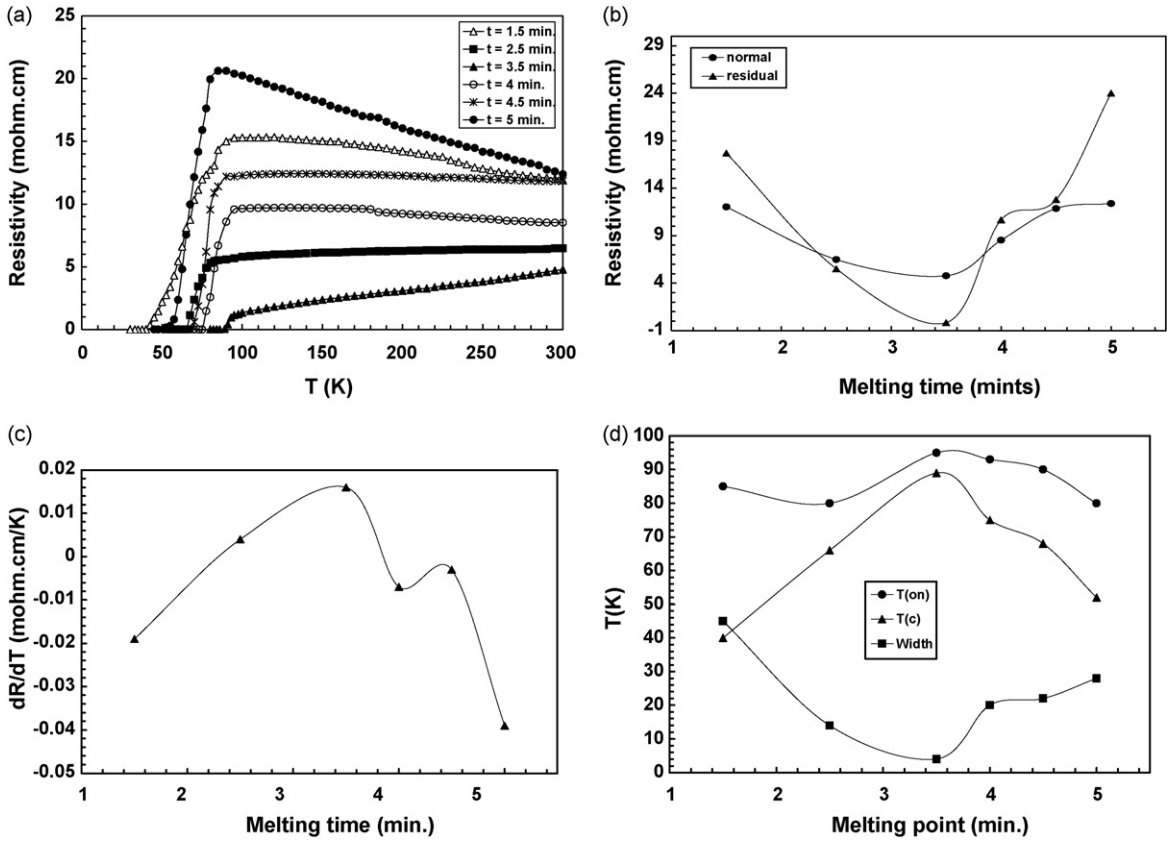

Fig. 4. (a) Resistivity versus temperature at different melting time for Bi (Pb): 2212 samples. (b) Normal and residual resistivities versus melting time for Bi (Pb): 2212 samples. (c) Resistivity-temperature slope versus melting time for Bi (Pb): 2212 samples. (d) T_c, $T_{(on)}$ and width of transition versus melting time for Bi (Pb): 2212 samples

time is controlled by the presence of oxygen vacancies during melting operation, which may affect the carrier concentration. This also may lead to lattice variations in Bi (Pb): 2212 system, as reported experimentally [24]. On the light of these observations, one can say that the presence of both oxygen vacancies and lattice variations in Bi (Pb): 2212 system may reduce the path of current flow in the system and eventually the superconductivity is improved.

On the other hand, the Hall effect of high temperature superconductors has been studied extensively in the normal and mixed states [14,25–27]. One of the most remarkable observations in the normal and mixed state is the unconventional behavior of the Hall effect. In the normal state above T_c, Hall coefficient measurements provide information on the sign, concentration and mobility of charge carriers. The most important result obtained from Hall effect measurements in the normal state is that the charge carriers in the copper-oxide planes are mostly holes. The only major exception from these high T_c superconductors is $Nd_{2-x}Ce_xCuO_4$ superconductors, with electron-like conduction [25]. The values of Hall number (R_h^{-1}) and carrier density (n) as a function of melting time are listed in Table 1, which are of typical behavior shown in microhardness and T_c. The values of Hall number are changed from 346 up to 662 with increasing melting time; where as the values of carrier density are changed from $2.16 \times 10^{21}/cm^3$ up to $4.15 \times 10^{21}/cm^3$. These values are found to be comparable with those reported for similar system in the under doped region [28–31].

The values of carrier density are utilized to estimate several normal state parameters such as Fermi energy E_f and density of states at Fermi level $N(E_f)$. E_f is given by [22]:

$$E_f = \left[\frac{\hbar^2(3\pi^2 n)^{3/2}}{2m^*}\right] \quad (3)$$

where $\hbar$ is the reduced Planks· constant and m^* is the effective mass of the carriers. We have taken $m^* = 3m_e$ for Bi: 2212 system [32,33]. While $N(E_f)$ is also given by [22]:

$$N(E_f) = \left(\frac{1}{2\pi^2}\right)\left(\frac{2m*}{\hbar^2}\right)^{3/2} E_f^{1/2} \quad (4)$$

The values of E_f and $N(E_f)$ are presented in Table 1 and show the same behavior against melting time as reported above. E_f values are changed from 0.132 eV up to 0.196 eV for the studied samples. These values are nearly comparable with those reported for La and Bi systems [22,34], and much smaller than those reported for conventional metals (5–10 eV). Actually, increasing E_f in the normal state region leads to a significant decrease in the electronic contribution to the total heat capacity and thermal conductivity. Thus, the lattice contribution to the heat capacity is expected to be large in such system. Moreover, the obtained values of $N(E_f)$ are comparable with those reported for the present system [33,35,36].

Anyhow, the high T_c Bi (Pb): 2212 system has been the consequence of the melting operation carried out at higher temperature. However, it has been indicated that a small depleting effect such as Bi-stoichiometry may result from the melting operation during the synthesis of the materials. This might lead to an increase in the effective Cu valance, which is known to be crucial for superconductivity [13,37]. Increasing T_c is accompanied by a reduced transition width, which may be the consequence of improved ordering of Bi-stoichiometry due to melting operation. The manifestation of such improved ordering is revealed by the enhancement in the measured and calculated parameters mentioned earlier. However, similar behavior is reported for suppression of dissipative flux motion by Dy doping in high T_c (Bi,Pb): 2212 superconductor [38]. Furthermore, a reduction of hole concentration, in the CuO_2 planes of

(Bi,Pb): 2212 system, is responsible for suppression of T_c by Ce substitution [39].

4. Conclusions

The impact of melting time (1.5–5 min) in air and at 920 °C on the normal and superconducting properties of Bi (Pb): 2212 system is reported here. The results of XRD, SEM, microhardness, resistivity and Hall coefficient measurements based on the considered samples are presented in details. Moreover, the density of holes, Fermi energy and density of states at Fermi level are also calculated and discussed for all studied samples. These results show a strong correlation between the behaviors of the above parameters against melting time, and indicate that the critical temperature T_c could be optimized at 89 K through melting operation at t = 3.5 min for the considered system.

Acknowledgment

The author would like to thank the Deanship of Scientific Research for providing facilities and maintenance support during the present project.

References

[1] H. Maeda, Y. Tanaka, M. Fukutomi, T. Asano, Jpn. J. Appl. Phys. 27 (1988) L209.
[2] Y. Yamada, T. Watanabe, M. Suzuki, Physica C 460–462 (2007) 815.
[3] A. Sedky, Physica C 468 (2008) 1041.
[4] A. Sedky, J. Phys. Chem. Solids 70 (2009) 483.
[5] K.M. Lang, V. Madhavan, J.E. Hoffman, E.W. Hudson, H. Eisaki, S. Uchida, J.C. Davis, Nature 415 (2002) 412.
[6] H. Eisaki, N. Kaneko, D.L. Feng, A. Damascelli, P.K. Mang, K.M. Shen, Z.X. Shen, M. Greven, Phys. Rev. B 69 (2004) 064512.
[7] F. Jean, G. Collin, M. Andrieux, N. Blanchard, J.F. Marucco, Physica C 339 (2000) 269.
[8] T. Yamamoto, I. Kakeya, K. Kadowaki, Physica C 460–462 (2007) 799.
[9] B. Reveau, C. Michael, F. Studr, J. Provost, M. Herveau, in: A.V. Narlikar (Ed.), Studies of High Temperature Superconductors, vol. 9, Nova Science, New York, 1992, p. 81.
[10] G.G. Qian, K.Q. Ruan, X.H. Chen, C.Y. Wang, L.Z. Cao, M.R. Ji, Physica C 313 (1999) 58.
[11] A. Sedky, A.M. Ahmed, Chinese J. Phys. 41 (5) (2003) 1.
[12] D.M. Pooke, G.V.M. Williams, Physica C 354 (2001) 396.
[13] S.K. Agarwal, V.P.S. Awana, V.N. Moorthy, P. Maruthi Kumar, B.V. Kumaraswamy, C.V.N. Rao, A.V. Narlikar, Physica C 160 (1989) 278.
[14] A.Q. Pham, A. Maignan, M. Hervieu, C. Michel, J. Provost, B. Raveau, Physica C 191 (1994) 77.
[15] M. Uehera, Y. Asada, H. Maeda, K. Ogawa, Jpn. J. Appl. Phys. 27 (1988) L665.
[16] S.M. Khalil, A. Sedky, Physica B 357 (2005) 299.
[17] M. Grayson Alexander, Phys. Rev. B 38 (1988) 91914.
[18] M. Gazda, B. Kusz, T. Klimczuk, R. Natali, S. Stizza, Physica C 460–462 (2007) 847.
[19] N. Panarina, D. Bizyaev, V. Petukhov, Yu. Talanov, Physica C 470 (2010) 251.
[20] T. Tamegai, K. Koga, K. Suzuki, M. Ichihara, F. Sakai, Y. Iye, Jpn. J. Appl. Phys. 28 (1989) L112.
[21] V.P.S. Awana, S.B. Samanta, P.K. Dutta, E. Gmelin, A.V. Narlikar, J. Phys. Condens. Matter 3 (1991) 8893.
[22] P. Mandal, A. Poddar, B. Ghosh, P. Choudhury, Phys. Rev. B 43 (16) (1991) 13102.
[23] S. Ravi, V. Seshu Bai, Phys. Rev. B 49 (1994) 13082.
[24] S. Kambe, T. Matsuoka, M. Takahasi, M. Kawai, T. Kawai, Phys. Rev. B 42 (1990) 2669.
[25] T. Nishikawa, J. Takeda, J. Sato, J. Phys. Soc. Jpn. 63 (1994) 1441.
[26] M. Matusiak, T. Plackowski, C. Sulkowski, H. Misiorek, Physica C 384 (2003) 237.
[27] A. Salem, G. Jakob, H. Adrian, Physica C 415 (2004) 62.
[28] C. Allgeier, J.S. Schilling, Physica C 168 (499) (1990) 499.
[29] J. Clayhold, S.J. Hagen, N.P. Ong, J.M. Tarascon, P. Barboux, Phys. Rev. B 39 (1989) 7320.
[30] T. Tamegai, K. Koga, K. Suzuki, M. Ichihara, F. Sakai, Y. Iye, Jpn. J. Appl. Phys. 28 (1998) L112.
[31] Y. Koika, Y. Iwabuchi, S. Hosoya, N. Kobayashi, T. Fukasa, Physica C 159 (1989) 105.
[32] K.N. Kishore, S. Satyavathi, M. Muralidhar, O. Pena, V.H. Babu, Physica C 252 (1995) 49.
[33] S. Tanaka, Phys. Scripta T 27 (1989) 7.
[34] V.Z. Kresin, S.A. Wolf, Phys. Rev. B 41 (1990) 4278.
[35] R.A. Fisher, S. Kim, S.E. Lacy, N.E. Phillips, D.E. Morris, A.G. Markelz, J.Y.T. Wei, D.S. Ginley, Phys. Rev. B 38 (1988) 11942.
[36] N. Okazaki, T. Hasegawa, K. Kishio, K. Kitazawa, A. Kishi, Y. Ikeda, M. Takano, K. Oda, H. Kitaguchi, J. Takada, Y. Miura, Phys. Rev. B 41 (1989) 4296.
[37] A.V. Narlikar, C.V. Narasimha Rao, S.K. Agarwal, Studies of High Superconductors, Vol. 1, Ed. A.V. Narlikar, Nova Science Publishers, NY, 1989, p. 341.
[38] P.M. Sarun, S. Vinu, R. Shabna, U. Syamaprasad, J. Alloys Compd. (2009), doi:10.1016/j.jallcow.2010.02.168.
[39] R. Shabna, P.M. Sarun, S. Vinu, U. Syamaprasad, J. Alloys Compd. 493 (2010) 11.